CHIN. PHYS. LETT. Vol. 32, No. 3 (2015) 037201

Enhancement of Thermoelectric Performance of $Sr_{0.9}Ba_{0.1}Ti_{0.8}Nb_{0.2}O_3$ Ceramics by A-Site Cation Nonstoichiometry *

ZHANG Xin(张鑫)[1,2], LIU Jian(刘剑)[1**], LI Yi(李宜)[1], SU Wen-Bin(苏文斌)[1], LI Ji-Chao(李吉超)[1], ZHU Yuan-Hu(祝元虎)[1], LI Mao-Kui(李茂奎)[1], WANG Chun-Ming(王春明)[1], WANG Chun-Lei(王春雷)[1]

[1]*School of Physics, State Key Laboratory of Crystal Materials, Shandong University, Jinan 250100*
[2]*Taishan College, Shandong University, Jinan 250100*

(Received 15 September 2014)

$Sr_{0.9}Ba_{0.1-x}Ti_{0.8}Nb_{0.2}O_3$ ceramics (x=0, 0.01, 0.02 and 0.05) are prepared by solid state reaction, whose thermoelectric properties are investigated from 323 K to 1073 K. By introducing A-site nonstoichiometry, the absolute Seebeck coefficient is enhanced, while the electrical resistivity is surprisingly reduced due to the significantly enhanced carrier mobility. These results are dramatic in thermoelectric materials, effectively enhancing the power factor. Moreover, the thermal conductivity is reduced, thus the thermoelectric performance of $Sr_{0.9}Ba_{0.1}Ti_{0.8}Nb_{0.2}O_3$ ceramic is significantly enhanced by A-site nonstoichiometry.

PACS: 72.20.Pa, 72.10.Fk, 74.62.Dh DOI: 10.1088/0256-307X/32/3/037201

Thermoelectric (TE) materials have attracted great interest because of their potential application in solid-state cooling and power generation from waste heat.[1−3] The performance of a TE material is evaluated by the figure-of-merit $ZT = S^2T/\rho\kappa$, where S, T, ρ and κ are the Seebeck coefficient, absolute temperature, electrical resistivity, and thermal conductivity, respectively. Recently, nonstoichiometry was found to be an effective approach to the enhancement of TE performance. Generally, nonstoichiometry is regarded as a scattering center of heat and electrical transports. The thermal conductivity would be reduced by introducing nonstoichiometry.[4−7] On the other hand, nonstoichiometry might change the carrier concentration, and thus influence the TE power factor ($PF = S^2/\rho$).[8−11] Oxygen nonstoichiometry is very important in the n-type TE oxides, such as $SrTiO_3$[8] and (Sr,Ba)Nb_2O_6,[9] to obtain a low electrical resistivity. By introducing Cu nonstoichiometry into BiCuSeO, both the electrical resistivity and Seebeck coefficient decrease, resulting in enhancements of the power factor and TE performance.[10] In these works, the effects of nonstoichiometry are similar to those of element substitution, acting as carrier donors, and the carrier concentration increases with the introduction of nonstoichiometry.

In this Letter, A-site nonstoichiometry was introduced into $Sr_{0.9}Ba_{0.1}Ti_{0.8}Nb_{0.2}O_3$ ceramics which exhibit the ABO_3 perovskite structure. Due to the simple valence analysis, A-site nonstoichiometry should reduce the electron concentration, thus enhancing the electrical resistivity and absolute Seebeck coefficient of $Sr_{0.9}Ba_{0.1}Ti_{0.8}Nb_{0.2}O_3$ ceramics. However, in this work, the electrical resistivity of $Sr_{0.9}Ba_{0.1-x}Ti_{0.8}Nb_{0.2}O_3$ ceramics surprisingly decreases with the introduction of A-site nonstoichiometry, accompanied with enhanced absolute Seebeck coefficient. Therefore, both the power factor and the figure-of-merit ZT are enhanced significantly.

$Sr_{0.9}Ba_{0.1-x}Ti_{0.8}Nb_{0.2}O_3$ (x = 0, 0.01, 0.02 and 0.05) ceramics were prepared by the reduced solid-state reaction techniques. The starting materials were Nb_2O_5 (with purity of 99.5%), TiO_2 (99.8%), $BaCO_3$ (99.8%), and $SrCO_3$ (99.8%). Appropriate amounts of the starting materials were weighted, mixed by ball-milling, and pressed into pellets. The pellets were then calcined in air for 6 h at 1350℃, and they were heated rapidly above 1000℃ with the heating rate of 10℃/min to avoid generation of the $Sr_5Nb_4O_{15}$ second phase.[12] After intermediate ball-milling and pressing, the obtained pellets were sintered at 1500℃ for 6 h in a forming gas of 5 mol% hydrogen in argon.

The crystal structure and lattice parameter were characterized by powder x-ray diffraction with Cu Kα radiation (λ = 0.154056 nm) utilizing a Rigaku D/MAX-2550P diffractometer. The surface microstructures were observed by a scanning electron microscope (SEM) system (Zeiss, SUPRA 55). The sintered pellets were cut into rectangular columns ($12 \times 2 \times 2\,mm^3$) for measurements of the electrical resistivity and Seebeck coefficient using a Linseis LSR-3/1100 instrument in a helium atmosphere by a dynamic method. The Hall Effect was measured at room temperature by an MMR M75-K25/6R instrument. The thermal conductivity was calculated from the thermal diffusivity, the specific heat capacity, and

*Supported by the National Basic Research Program of China under Grant No 2013CB632506, the National Natural Science Foundation of China under Grant Nos 51202132, 51002087 and 11374186, and the Independent Innovation Foundation of Shandong University under Grant No IIFSDU 2012TS028.

**Corresponding author. Email: liujjx@sdu.edu.cn

© 2015 Chinese Physical Society and IOP Publishing Ltd

the sample density measured on a laser flash apparatus (Netzsch LFA 427), a thermal analyzer (Netzsch STA 449C), and by Archimedes' method, respectively.

The powder x-ray diffraction (XRD) patterns of all of the samples are shown in Fig. 1. According to the PDF card, all of the samples are of single phase in a cubic structure. The lattice parameters were obtained from the results of XRD, as listed in Table 1, which decrease with the introduction of A-site nonstoichiometry. The decrease of lattice parameter can be attributed to the absence of ions at A-sites of the lattice. The theoretical densities of all of the samples were calculated from the lattice parameters, and the bulk densities were measured by Archimedes' method, as listed in Table 1. The relative density increases with the introduction of nonstoichiometry, showing that A-site nonstoichiometry is beneficial to produce dense ceramics.

Table 1. The lattice parameters a, measured bulk density $\rho_{\rm m}$, theoretical density $\rho_{\rm th}$ and relative density $\rho_{\rm r}$ of all of the samples.

	a (nm)	$\rho_{\rm m}$ (g/cm^3)	$\rho_{\rm th}$ (g/cm^3)	$\rho_{\rm r}$ (%T.D.)
$x = 0$	0.3941	5.04	5.36	94.0
$x = 0.01$	0.3938	5.07	5.33	95.1
$x = 0.02$	0.3934	5.18	5.31	97.6
$x = 0.05$	0.3926	5.11	5.23	97.7

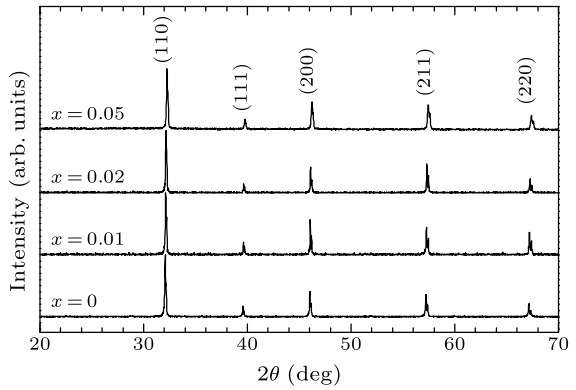


Fig. 1. The x-ray diffraction patterns of $Sr_{0.9}Ba_{0.1-x}Ti_{0.8}Nb_{0.2}O_3$ ($x = 0$, 0.01, 0.02 and 0.05) powders.

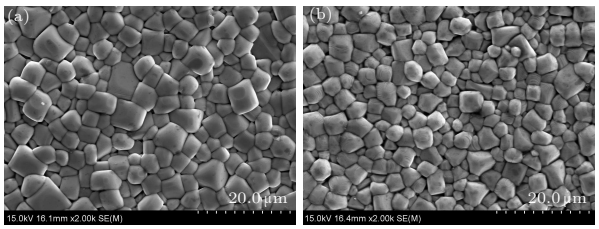


Fig. 2. SEM images of $Sr_{0.9}Ba_{0.1-x}Ti_{0.8}Nb_{0.2}O_3$ ceramics: (a) $x = 0$ and (b) $x = 0.02$.

Figure 2 shows the SEM images of the surfaces of $Sr_{0.9}Ba_{0.1-x}Ti_{0.8}Nb_{0.2}O_3$ ($x = 0$ and 0.02) ceramics. Both samples exhibit dense microstructures with no pores. With the introduction of nonstoichiometry, the average grain size slightly decreases from ~3.3 μm of the sample $x = 0$ to ~2.9 μm of the sample $x = 0.02$.

The temperature dependences of Seebeck coefficient (S) of $Sr_{0.9}Ba_{0.1-x}Ti_{0.8}Nb_{0.2}O_3$ ($x = 0$, 0.01, 0.02 and 0.05) ceramics are shown in Fig. 3. The Seebeck coefficients of all of the samples are negative and decrease monotonically with increasing temperature, showing n-type metallic behavior.[8,13,14] The magnitude of absolute Seebeck increases when more vacancies are introduced into the A-sites. Generally, the increase of absolute S is attributed to the decrease of carrier concentration in a rigid-band model, which is normally accompanied with an increase of electrical resistivity. According to the simple valence analysis, one A-site vacancy would take two electrons away. Therefore, A-site nonstoichiometry is reasonable for the decrease of electron concentration, and thus the increase of absolute Seebeck coefficient.

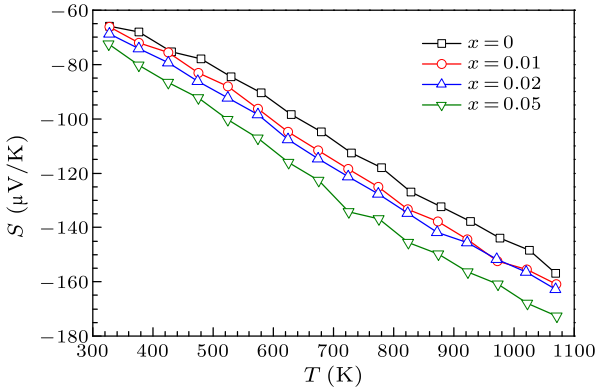


Fig. 3. Temperature dependence of Seebeck coefficient of $Sr_{0.9}Ba_{0.1-x}Ti_{0.8}Nb_{0.2}O_3$ ($x = 0$, 0.01, 0.02 and 0.05) ceramics.

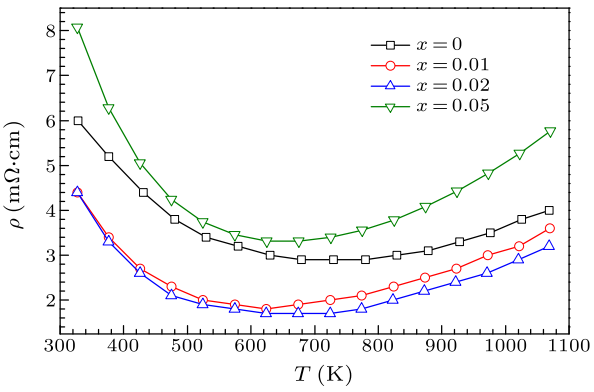


Fig. 4. Temperature dependence of electrical resistivity of $Sr_{0.9}Ba_{0.1-x}Ti_{0.8}Nb_{0.2}O_3$ ($x = 0$, 0.01, 0.02 and 0.05) ceramics.

However, the magnitude of electrical resistivity is surprisingly reduced by slightly A-site nonstoichiometry, as shown in Fig. 4, which is inconsistent with valence analysis in the rigid band model. To clarify the origin of this anomaly, the Hall coefficients of all of the samples were measured at room temperature, and the carrier concentrations n and mobility

μ were subsequently calculated, as listed in Table 2. The carrier concentration is reduced with the introduction of A-site nonstoichiometry, which is consistent with the valence analysis and the increase of absolute S. However, the carrier mobility is enhanced significantly, thus the electrical resistivity decreases. The magnitude of electrical resistivity increases again when the content of A-site vacancies is large (in the sample $x = 0.05$), due to the fact that the decrease of carrier concentration plays a major role in this sample. How the carrier mobility is enhanced is still an open question. One possibility is the decrease of effective mass due to the change of band structure. Further detailed investigation on the carrier mobility and the band structure will be performed by *ab initio* calculation in the future.

Table 2. The carrier concentration n, electrical resistivity ρ_{300}, and carrier mobility μ of all the samples at 300 K.

	n (10^{20} cm^{-3})	ρ_{300} (mΩ·cm)	μ (cm^2/Vs)
$x = 0$	5.66	6.64	1.66
$x = 0.01$	3.07	5.41	3.76
$x = 0.02$	1.63	5.29	7.25
$x = 0.05$	0.77	9.86	8.19

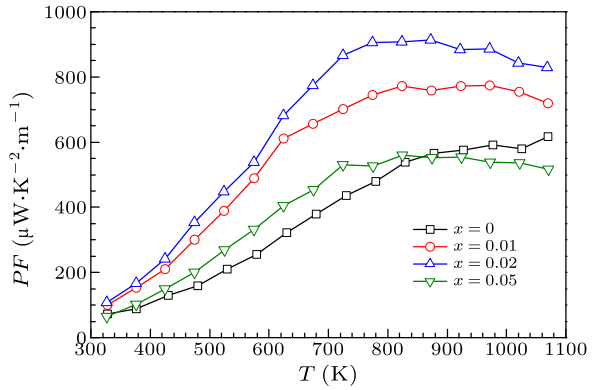


Fig. 5. Temperature dependence of power factor of $Sr_{0.9}Ba_{0.1-x}Ti_{0.8}Nb_{0.2}O_3$ (x = 0, 0.01, 0.02 and 0.05) ceramics.

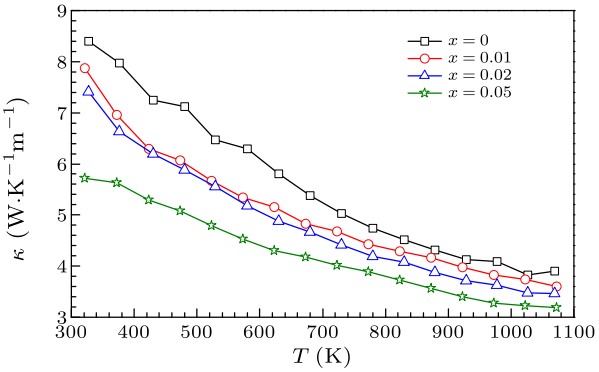


Fig. 6. Temperature dependence of thermal conductivity of $Sr_{0.9}Ba_{0.1-x}Ti_{0.8}Nb_{0.2}O_3$ (x = 0, 0.01, 0.02 and 0.05) ceramics.

According to the obtained electrical resistivity and Seebeck coefficient, the power factors $PF = S^2/\rho$ of all the samples were calculated, as shown in Fig. 5. The power factors of all of the samples increase with increasing temperature and show a broad peak at high temperatures. The magnitude of the power factor is enhanced significantly by slightly introducing A-site nonstoichiometry due to the simultaneously improved Seebeck coefficient and electrical conductivity. The maximum PF value is improved from 616 μW/K^{2}m ($x = 0$) to 914 μW/K^{2}m ($x = 0.02$).

The temperature dependences of thermal conductivity of all of the samples are shown in Fig. 6. The thermal conductivity of all of the samples decreases with the increase of temperature, dominated by the lattice contribution.[15] The magnitude of thermal conductivity decreases monotonously with the increasing content of nonstoichiometry, which could be attributed to the phonon scattering by point defects introduced by A-site vacancies.

Figure 7 shows the temperature dependence of the figure of merit (ZT). The ZT values of all of the samples increase with temperature in the whole temperature range. The TE performance is enhanced significantly by slightly introducing A-site nonstoichiometry due to the enhanced power factor and the reduced thermal conductivity, and then decreases due to the decrease of power factor in the heavily nonstoichiometric sample. The maximum ZT value is obtained in sample $x = 0.02$ to be 0.26 at 1073 K, enhanced by a factor of 53% over that of the stoichiometric one (0.17 at 1073 K). This shows that A-site nonstoichiometry is an effective way to improve the TE performance of $Sr_{0.9}Ba_{0.1}Ti_{0.8}Nb_{0.2}O_3$ ceramics.

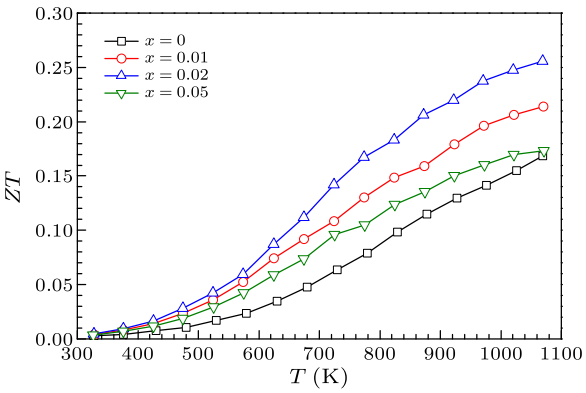


Fig. 7. Temperature dependence of dimensionless figure-of-merit ZT of $Sr_{0.9}Ba_{0.1-x}Ti_{0.8}Nb_{0.2}O_3$ (x = 0, 0.01, 0.02 and 0.05) ceramics.

In summary, a new approach has been reported in this work to improve the TE performance of oxide ceramics. By introducing A-site nonstoichiometry, the TE performance of $Sr_{0.9}Ba_{0.1}Ti_{0.8}Nb_{0.2}O_3$ ceramics is significantly enhanced. The absolute Seebeck coefficient increases, accompanied with a decrease of the electrical resistivity. Therefore, the TE

power factor is enhanced significantly. These special behaviors are mainly due to the dramatically enhanced carrier mobility. Meanwhile, the thermal conductivity is reduced due to the phonon scattering of point defects at A-sites. Therefore, the TE figure-of-merit ZT is enhanced and reaches the maximum value of 0.26 at 1073 K for the nonstoichiometric $Sr_{0.9}Ba_{0.08}Ti_{0.8}Nb_{0.2}O_3$ ceramic, which is improved by a factor of 53% over that of the stoichiometric one (0.17 at 1073 K). Such a nonstoichiometric method might be extended to other TE materials as a new way to improve TE performance.

References

[1] Bell L E 2008 *Science* **321** 1457
[2] Li J F, Liu W S, Zhao L D and Zhou M 2010 *NPG Asia Mater.* **2** 152
[3] Biswas K, He J Q, Blum I D, Wu C I, Hogan T P, Seidman D N, Dravid V P and Kanatzidis M G 2012 *Nature* **489** 414
[4] Pei Y Z and Morelli D T 2009 *Appl. Phys. Lett.* **94** 122112
[5] Zhu G H, Lan Y C, Wang H, Joshi G, Hao Q, Chen G and Ren Z F 2011 *Phys. Rev.* B **83** 115201
[6] Zhu T J, Zhang S N, Yang S H and Zhao X B 2010 *Phys. Status Solidi* RRL **4** 317
[7] Ji H S, Kim H, Lee C, Rhyee J S, Kim M H, Kaviany M and Shim J H 2013 *Phys. Rev.* B **87** 125111
[8] Liu J, Wang C L, Su W B, Wang H C, Zheng P, Li J C, Zhang J L and Mei L M 2009 *Appl. Phys. Lett.* **95** 162110
[9] Lee S, Wilke R H T, McKinstry S T, Zhang S J and Randall C A 2010 *Appl. Phys. Lett.* **96** 031910
[10] Liu Y, Zhao L D, Liu Y C, Lan J L, Xu W, Li F, Zhang B P, Berardan D, Dragoe N, Lin Y H, Nan C W, Li J F and Zhu H M 2011 *J. Am. Chem. Soc.* **133** 20112
[11] Chen L, Che G C, Li H, Dong C, Zhou F, Huang Y Z and Zhao Z X 2000 *Chin. Phys. Lett.* **17** 601
[12] Ianculescu A, Brãileanu A, Zaharescu M, Guillemet S, Pasuk I, Madarász J and Pokol G 2003 *J. Therm. Anal. Calorim.* **72** 173
[13] Muta H, Kurosaki K and Yamanaka S 2004 *J. Alloys Compd.* **368** 22
[14] Yamamoto M, Ohta H and Koumoto K 2007 *Appl. Phys. Lett.* **90** 072101
[15] Ohta H 2007 *Mater. Today* **10** 44